Intramembrane Positions of Membrane-Bound Chromophores Determined by Excitation Energy Transfer†

Dennis E. Koppel,* Patrick J. Fleming,‡ and Philipp Strittmatter

ABSTRACT: A detailed theory has been derived to evaluate the efficiency of nonradiative transfer of electronic excitation energy between nonassociated membrane-bound chromophores. Two different approaches are presented and shown to lead to identical numerical results. In the first of these, the efficiency of transfer is computed from the decay with time of the donor excited state. In the second approach, the efficiency is calculated directly, demonstrating that to a high degree of accuracy the array of acceptors can be represented as consisting of a single nearest acceptor plus a continuum of secondary acceptors. A general expression is derived for the dipole–dipole orientation factor as a function of the position of an acceptor. It is shown that, by invoking the range of orientations that must be present at the very least in a particular case, the expected values of transfer efficiency may be limited to a relatively narrow band of uncertainty about those predicted for total randomization. In the limit of total randomization, the theory reduces to functions of but two dimensionless parameters: an effective number of acceptors and a normalized distance of closest approach, a parameter which in turn is a function of an excluded surface area and the depth in the membrane of a donor relative to that of an acceptor. Finally, data analysis procedures are presented whereby one can determine the surface density of acceptors for a known geometry or, alternatively, determine the distance of closest approach for known surface densities.

Nonradiative transfer of electronic excitation energy has been applied to many problems in molecular biology as a means of estimating intramolecular distances in macromolecules [for a recent review, see Stryer (1978)]. In conventional experiments of this type, one seeks to attach a single donor (a fluorophore) and a single acceptor (a chromophore with an absorption spectrum overlapping the donor emission spectrum) to specific sites on the macromolecule. From the efficiency of transfer, E, measured under these conditions, one determines the distance between the donor and acceptor groups relative to R_0, the Förster critical distance (Förster, 1948).

The object of this paper is to provide a theoretical framework for the interpretation of energy transfer experiments in which transfer occurs between distinct nonassociated molecules in reconstituted model membrane systems. Emphasis is placed on the determination of the distance of closest approach of an acceptor to a donor, a parameter which in turn is a function of an excluded surface area and the depth in the membrane of a donor relative to that of an acceptor.

Each donor in the membrane system sees an array of many possible acceptors. Förster (1949) has derived a solution for a similar problem, that of a donor and acceptors randomly distributed in solution. Recently, Shaklai et al. (1977) and Fung & Stryer (1978) have adapted Förster's theory to the restricted membrane geometry with the principal objective of determining the surface densities of acceptors. In this approach, it is assumed from the start that all donor–acceptor pairs have the same R_0, i.e., that relative orientations are totally random and "dynamically" averaged during the excited-state lifetime of the donor. This is clearly a good assumption for the rapid isotropic rotations occurring in solution but is less obviously so for the relatively slow anisotropic rotations possible for membrane-bound probes. In the theory presented below, a general expression is derived for the dipole–dipole orientation factor as a function of the position of the acceptor, incorporating information, available from polarization measurements, on the amount of dynamic averaging that does exist in a particular case. It is shown that, by invoking the range of orientations that must be present at the very least in the membrane environment, expected values of E can be limited to a relatively narrow band of uncertainty about those predicted for total randomization.

An alternative approach is also presented below in which E is calculated directly, bypassing an intermediate calculation of $\rho(t)$, the decay of the donor excited state. The direct calculation of E has important practical advantages in the analysis of steady-state fluorescence data and also provides some useful physical insight into the nature of the array of acceptors.

In the limit of uniform R_0, general expressions are derived for $\rho(t)$ and E as functions of two dimensionless parameters. An empircal formula is presented that gives an accurate representation of E for wide ranges of these parameters, providing a simple analytical procedure for data analysis.

The following paper (Fleming et al., 1979) reports an experimental study of transfer from an intrinsic fluorescent tryptophanyl residue of cytochrome b_5 to extrinsic acceptor molecules in the polar head group region of phospholipid vesicles. Data analysis yields the depth in the bilayer of the donor residue. The distance thus determined can be used in this case to put constraints on the possible tertiary structure of the nonpolar segment of cytochrome b_5 and its orientation in phospholipid vesicles.

Theory

A theoretical analysis of excitation energy transfer between nonassociated membrane-bound chromophores is presented in the following sections. The first section (Energy Transfer to a Fixed Configuration of Acceptors) defines the geometry of the vesicle system and introduces the basic expressions for energy transfer to an array of acceptors. The analysis explicitly includes the effects of averaging over rapid reorientations during the lifetime of the donor excited state ("dynamic" averaging) but does not consider the averaging of motions over

† From the Department of Biochemistry, University of Connecticut Health Center, Farmington, Connecticut 06032. *Received April 26, 1979; revised manuscript received September 6, 1979.* This investigation was supported by Research Grants GM23585 and GA15924 from the U.S. Public Health Service.

‡ Recipient of National Institutes of Health Postdoctoral Fellowship 1 G32 GM 05803-01. Present address: Department of Biochemistry, Georgetown University Schools of Medicine and Dentistry, Washington, D.C. 20007.

0006-2960/79/0418-5450$01.00/0 © 1979 American Chemical Society

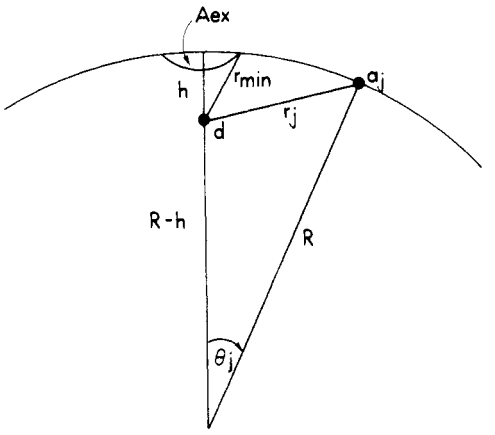

FIGURE 1: Assumed geometry of the model membrane system. d and a_j indicate the positions of the donor and the jth acceptor, respectively.

longer time scales ("static" or ensemble averaging). Ensemble averaging is effected in the next section (Ensemble Averaging) for two different formulations: a derivation of $\langle\rho(t)\rangle$, the ensemble average of the decay of the donor excited state, and a direct derivation of $\langle E\rangle$, the ensemble average of the energy transfer efficiency. Each are expressed as functions of $\langle\overline{\kappa^2}\rangle_{A_j}$, the ensemble and dynamically averaged dipole–dipole orientation factor. A general expression for $\langle\overline{\kappa^2}\rangle_{A_j}$ as a function of the position of the acceptor is then derived in the following section (The Orientation Factor), incorporating the range of orientations that are known to be present at the very least. In the last section (A Useful Limiting Case) the theory is evaluated in the more familiar limit in which it is assumed that all donor–acceptor pairs have the same orientation factor. In the Appendix (Evaluation of Correction Terms), an evaluation is presented of the possible effects of an approximation made in the theoretical derivation.

Energy Transfer to a Fixed Configuration of Acceptors. Figure 1 defines the geometry of our model membrane system. The donors and acceptors are assumed to lie on spherical shells of radius $R - h$ and R, respectively, each confined to one or the other of the monolayers of the bilayer vesicle. Thus, h is the depth in the membrane of the donor relative to the acceptor. In general, h can be positive or negative. It is further assumed that acceptors are physically excluded from an area A_{ex} associated with each donor. Otherwise, the acceptors are randomly distributed among the vesicles and on the surface of each vesicle.

Consider one of the donors surrounded by an array of acceptors. E, the efficiency of energy transfer, is defined as the probability that a deexcitation of the donor will be coupled to the excitation of an acceptor. In the very weak, dipole–dipole coupling limit, γ_j, the instantaneous probabilistic rate of transfer to the jth acceptor relative to the deexcitation rate in the absence of acceptors, is given by (Förster, 1948)

$$\gamma_j = \beta\kappa_j^2/r_j^6 \tag{1}$$

β is a constant for a given donor–acceptor combination that depends in the usual way upon the fluorescence quantum efficiency of the donor in the absence of transfer, the integral of spectral overlap between the normalized donor emission spectrum and the acceptor absorption spectrum, and the index of refraction of the medium. κ_j^2 is an orientation factor with the form

$$\kappa_j^2 = [\hat{D}\cdot\hat{A} - 3(\hat{D}\cdot\mathbf{r}_j)(\hat{A}\cdot\mathbf{r}_j)/r_j^2]^2 \tag{2}$$

where $\hat{D}$, $\hat{A}$, and $\mathbf{r}_j/r_j$ are unit vectors which lie along the donor and acceptor transition moments and the direction joining them respectively. The magnitude of $\mathbf{r}_j$ is simply related to R, $R - h$, and θ_j (see Figure 1) by the law of cosines. It will later prove convenient to specify the position of the jth acceptor by $A_j = 2\pi R^2(1 - \cos\theta_j)$, the area at radius R of the "cap" subtended by a cone of half-angle θ_j. In this notation

$$r_j^2 = h^2 + \frac{R - h}{R}\frac{A_j}{\pi} \tag{3}$$

The rate of transfer to an array of acceptors is the sum of that to each individual acceptor. For a particular configuration of acceptors, $\rho(t)$, the probability that a donor excited at $t = 0$ is still excited at time t, has the form [compare with eq 6 of Förster (1949)]

$$\rho(t) = \exp\left[-\frac{t}{\tau_0}(1 + \sum_j \bar{\gamma}_j)\right] \tag{4}$$

where τ_0 is the excited-state lifetime of the donor in the absence of acceptor, and

$$\bar{\gamma}_j \equiv \frac{1}{t}\int_0^t \gamma_j(t')\,dt' \tag{5}$$

represents a "dynamic" averaging of γ_j over times comparable to the excited-state lifetime. Throughout this analysis we shall assume that r_j does not change during the excited-state lifetime of the donor but that the orientation factor, κ_j, has a component that does.

The efficiency of energy transfer is given by

$$E = 1 - \frac{1}{\tau_0}\int_0^\infty \rho(t)\,dt \tag{6}$$

By eq 4, this reduces to

$$E = \frac{\Gamma}{1 + \Gamma} \tag{7}$$

where

$$\Gamma \equiv \sum_j \bar{\gamma}_j \tag{8}$$

Keep in mind that, up until this point, the equations derived are only for a particular configuration of acceptors, i.e., for particular values of the r_j and $\overline{\kappa_j^2}$ for each acceptor. Expressions for $\langle\rho(t)\rangle$ and $\langle E\rangle$, averaged over the ensemble of configurations, are derived below. Ensemble averaging can be considered as a "static" averaging over variables that change on time scales long compared to the excited-state lifetime.

Ensemble Averaging. (1) Decay of the Excited State. An expression for the ensemble average of $\rho(t)$ can be derived from eq 4 by manipulations analogous to those of Förster (1949) [see also Shaklai et al. (1977)]. This leads to[1] the equation

$$\langle\rho(t)\rangle = \exp\left\{-t/\tau_0 - \sigma\int_{A_{ex}}^{A}[1 - \langle\exp(-\bar{\gamma}_j t/\tau_0)\rangle_{A_j}]\,dA_j\right\} \tag{9}$$

where σ is the average surface density of acceptor, $A = 4\pi R^2$ is the total surface area, and the subscript A_j, outside the angular ensemble average brackets, indicates that A_j is held constant within. To proceed further we perform a Taylor expansion of $\exp(-\bar{\gamma}_j t/\tau_0)$ in $\bar{\gamma}_j$ about $\bar{\gamma}_j = \langle\bar{\gamma}_j\rangle_{A_j}$. Substituting back into eq 9, the term linear in $\delta\bar{\gamma}_j$ averages to zero, leaving

$$\langle\exp(-\bar{\gamma}_j t/\tau_0)\rangle_{A_j} = \exp(-\langle\bar{\gamma}_j\rangle_{A_j} t/\tau_0) + \frac{1}{2}((\langle\bar{\gamma}_j\rangle_{A_j} t/\tau_0)^2\mu_j^2\exp(-\langle\bar{\gamma}_j\rangle_{A_j} t/\tau_0) + \ldots \tag{10}$$

[1] It is worth noting, for possible future reference, that eq 9 can be derived without invoking an effectively infinite vesicle size. It is enough to assume that the number of acceptors per vesicle is Poisson distributed, a fact that follows directly from the assumption that the acceptor molecules are randomly distributed among the vesicles.

where, in the first correction term

$$\mu_j^2 \equiv \langle(\overline{\delta\kappa_j^2})^2\rangle_{A_j}/\langle\overline{\kappa_j^2}\rangle_{A_j}^2 \quad (11)$$

is the normalized second moment of $\overline{\kappa_j^2}$ about its average. As will be shown in the Appendix, to a good approximation, this correction term can be neglected as well. Note that the averaged orientation factor, $\langle\overline{\kappa_j^2}\rangle_{A_j}$, is an explicit function of the location of the acceptor. This is true in the general case as a result of the anisotropic rotations of membrane-bound probes. A general expression for $\langle\overline{\kappa_j^2}\rangle_{A_j}$ is derived below (see The Orientation Factor).

(*2*) *Transfer Efficiency.* As an alternative to the derivation of the previous section, one can use eq 7 as the basis for a direct calculation of $\langle E\rangle$. We note, first of all, that because of the sharp drop-off of γ_j with increasing r_j one would expect that the nearest acceptors to a given donor would have a predominant effect on the total transfer efficiency. We single out the nearest acceptor for special consideration and designate it $j = 1$. Each configuration of acceptors is classified by its particular value of A_1, with A_1 employed as a subscript to indicate that consideration is limited to that particular class of configuration. The ensemble average of E can then be written as

$$\langle E\rangle = \int_{A_{ex}}^{A}\left\langle\frac{\Gamma}{1+\Gamma}\right\rangle_{A_1} P(A_1)\,dA_1 \quad (12)$$

where $P(A_1)dA_1$ is the probability that the nearest acceptor is at a position corresponding to a subtended area A_1, within dA_1. For a random distribution of acceptors excluded from the area A_{ex}, the number of acceptors within the boundaries of A_j is Poisson distributed about an average of $\sigma(A_j - A_{ex})$. Hence

$$P(A_1)dA_1 = \exp[-\sigma(A_1 - A_{ex})]\sigma dA_1 \quad (13)$$

As above, we can express $\Gamma/(1+\Gamma)$ as a Taylor expansion in Γ about $\langle\Gamma\rangle_{A_1}$. Substituting back into eq 12, the term linear in $\delta\Gamma$ averages to zero, and to a good approximation (see Appendix)

$$\langle E\rangle = \sigma\int_{A_{ex}}^{A}\frac{\langle\Gamma\rangle_{A_1}}{1+\langle\Gamma\rangle_{A_1}}\exp[-\sigma(A_1 - A_{ex})]\,dA_1 \quad (14)$$

Γ (see eq 8) can be divided into two parts: the contribution of the nearest acceptor ($A_j = A_1$) and that of all secondary acceptors ($A_j > A_1$). Thus

$$\langle\Gamma\rangle_{A_1} = \langle\bar{\gamma}_1\rangle_{A_1} + \sigma\int_{A_1}^{A}\langle\bar{\gamma}_j\rangle_{A_j}\,dA_j \quad (15)$$

where averaging over the positions of all secondary acceptors is accomplished by considering them as a homogeneous distribution of surface density σ.

Orientation Factor. The objective of this section is to derive a general expression for $\langle\overline{\kappa_j^2}\rangle_{A_j}$ for the specific geometry under consideration. The distinguishing feature of the vesicle system, as far as the orientation factor is concerned, is the fact that the molecules containing the donor and acceptor groups are free to rotate within the plane of the membrane about directions normal to the membrane surface. These extra degrees of freedom act to reduce the range of the possible values of $\langle\overline{\kappa_j^2}\rangle_{A_j}$.

The instantaneous position of $\hat{D}$ is specified in spherical coordinates by equatorial angle θ_D and azimuthal angle ϕ_D relative to a set of axes, $\hat{x}_D$, $\hat{y}_D$, and $\hat{z}_D$, with $\hat{z}_D$ defined as being normal to the membrane surface at the position of the donor. Thus

$$\hat{D} = \sin\theta_D\cos\phi_D\,\hat{x}_D + \sin\theta_D\sin\phi_D\,\hat{y}_D + \cos\theta_D\,\hat{z}_D \quad (16)$$

An equivalent relation holds for $\hat{A}$ in terms of θ_A, ϕ_A, $\hat{x}_A$, $\hat{y}_A$, and $\hat{z}_A$, with the $\hat{z}_A$ axis normal to the membrane surface at the position of the acceptor and hence at the angle θ_j relative to $\hat{z}_D$. Without loss of generality, we can orient these two sets of axes about $\hat{z}_D$ and $\hat{z}_A$ so that $\mathbf{r}_j$ lies within both the $\hat{y}_D$,$\hat{z}_D$ and the $\hat{y}_A$,$\hat{z}_A$ planes. In this case

$$\mathbf{r}_j = y_j\hat{y}_D + z_j\hat{z}_D \quad (17)$$

where

$$y_j = R\sin\theta_j$$

$$z_j = R\cos\theta_j - (R - h)$$

and

$$\hat{A} = \sin\theta_A\cos\phi_A\,\hat{x}_D + (\sin\theta_j\cos\theta_A + \cos\theta_j\sin\theta_A\sin\phi_A)\hat{y}_D + (\cos\theta_j\cos\theta_A + \sin\theta_j\sin\theta_A\sin\phi_A)\hat{z}_D \quad (18)$$

Substituting eq 16–18 into eq 2, averaging over θ_D and θ_A, and the uniform distributions of ϕ_D and ϕ_A, gives $\langle\overline{\kappa_j^2}\rangle$ as a function of $\langle\overline{\cos^2\theta_D}\rangle$, $\langle\overline{\cos^2\theta_A}\rangle$, θ_j, R, and h:

$$\langle\overline{\kappa_j^2}\rangle_{A_j} = \langle\overline{\cos^2\theta_D}\rangle\langle\overline{\cos^2\theta_A}\rangle a_{VV} + \langle\overline{\cos^2\theta_D}\rangle\times\langle\overline{\sin^2\theta_A}\rangle a_{VH} + \langle\overline{\sin^2\theta_D}\rangle\langle\overline{\cos^2\theta_A}\rangle a_{HV} + \langle\overline{\sin^2\theta_D}\rangle\langle\overline{\sin^2\theta_A}\rangle a_{HH} \quad (19)$$

where

$$a_{VV} = [\cos\theta_j - 3z_j(z_j\cos\theta_j + y_j\sin\theta_j)/r_j^2]^2 \quad (20a)$$

$$a_{VH} = (1/2)[\sin\theta_j - 3z_j(z_j\sin\theta_j - y_j\cos\theta_j)/r_j^2]^2 \quad (20b)$$

$$a_{HV} = (1/2)[\sin\theta_j - 3y_j(y_j\sin\theta_j + z_j\cos\theta_j)/r_j^2]^2 \quad (20c)$$

$$a_{HH} = (1/4)\{1 + [\cos\theta_j - 3y_j(y_j\cos\theta_j - z_j\sin\theta_j)/r_j^2]^2\} \quad (20d)$$

The orientation factor is seen to be a weighted average of the functions a_{VV}, a_{VH}, a_{HV}, and a_{HH}. The subscripts stand for "vertical" and "horizontal". Thus, for example, $\langle\overline{\kappa_j^2}\rangle_{A_j} = a_{VH}$ when the donor is "vertical" (i.e., $\hat{D}$ is perpendicular to the membrane surface so that $\langle\overline{\cos^2\theta_D}\rangle = 1$), and the acceptor is "horizontal" (i.e., $\hat{A}$ is tangential to the membrane surface so that $\langle\overline{\sin^2\theta_A}\rangle = 1$).

To calculate systematic estimates of $\langle\overline{\cos^2\theta_D}\rangle$ and $\langle\overline{\cos^2\theta_A}\rangle$ and, hence, $\langle\overline{\kappa_j^2}\rangle_{A_j}$, we need a model for the rotational motion of the transition dipoles. For convenience, we adopt the approach established by Dale & Eisinger (1974). It is assumed that on a time scale short compared to the excited-state lifetime of the donor each transition dipole is free to rotate rapidly about some axis, with a uniform azimuthal distribution, over a limited range of equatorial angles. Physically, one can associate these rapid rotations with the motions of the chromophore groups about one or more single bonds. They lead to dynamic averaging (see eq 5) and can be calibrated with independent measurements of fluorescence depolarization.[2] Calculations have been performed (Dale & Eisinger, 1974) for different fixed orientations of the axes about which these rapid rotations occur. In our case, we can specify that these rotation axes themselves are free to rotate and must be uniformly distributed azimuthally about axes normal to the membrane surface. These rotations are slower and can be associated with motions of the entire macromolecule which

[2] Depolarization resulting from transition dipoles of mixed polarization can also be included as a dynamic averaging effect (Haas et al., 1978).

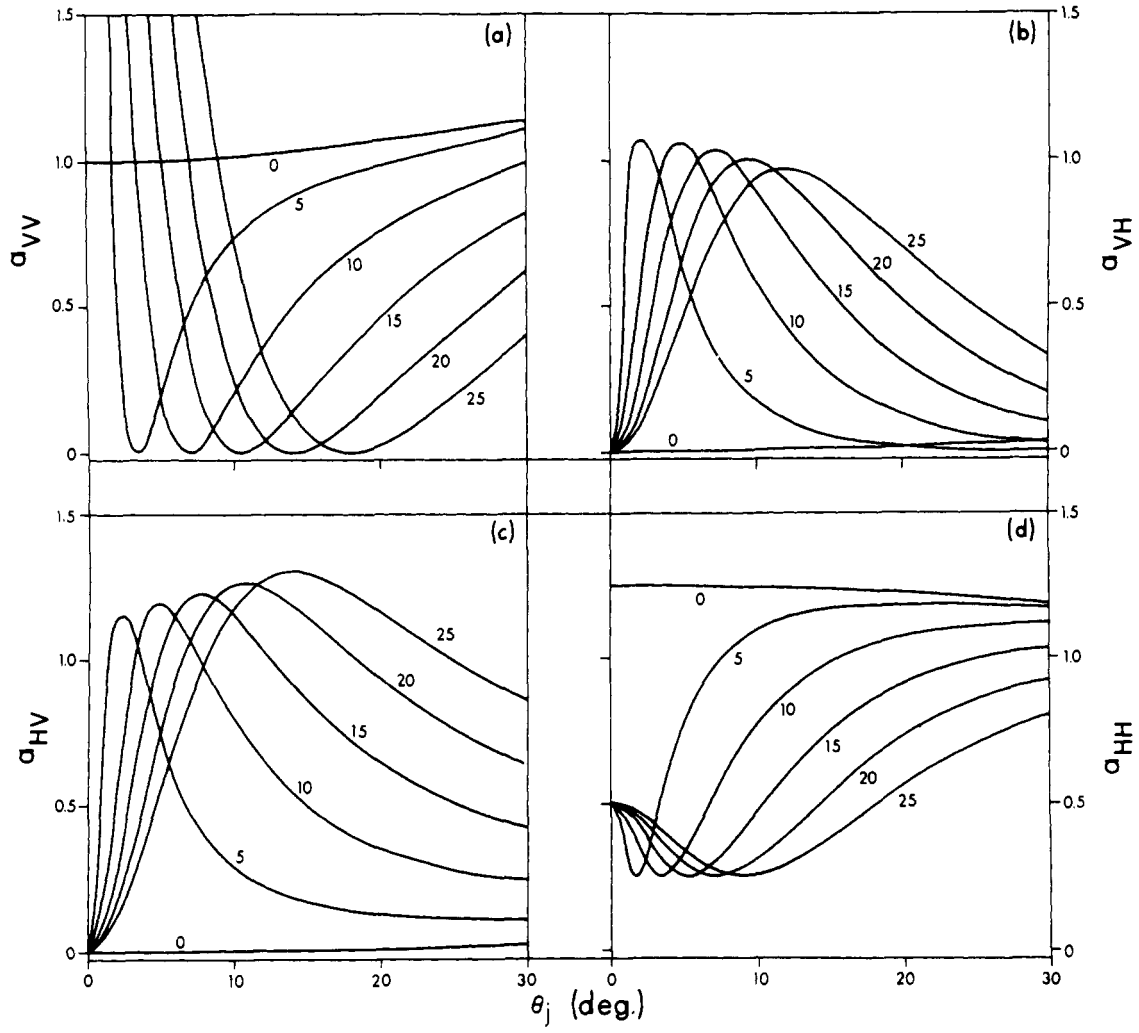

FIGURE 2: Theoretical values of a_{VV}, a_{VH}, a_{HV}, and a_{HH} calculated as functions of equatorial angle θ_j (i.e., the position of the acceptor) in a vesicle with R = 125 Å. The numbers associated with each curve indicate selected values of h in angstroms.

contains the chromophore group. Averaging over these additional degrees of freedom is incorporated in the static ensemble average.

The complete calculation requires the introduction of two additional sets of axes. We specify that $\hat{D}$ rotates rapidly about the $\hat{z}_D'$ axis. The instantaneous position of $\hat{D}$ relative to $\hat{x}_D'$, $\hat{y}_D'$, and $\hat{z}_D'$ is characterized in spherical coordinates by equatorial angle θ_D' and azimuthal angle ϕ_D'. It then follows that

$$\cos\theta_D = \hat{z}_D \cdot \hat{D} = \sin\theta_D' \sin\theta_D'' \sin\phi_D' + \cos\theta_D' \cos\theta_D'' \tag{21}$$

where θ_D'' is the equatorial angle of $\hat{z}_D'$ relative to $\hat{z}_D$. Averaging over the dynamic and static distributions, finally, gives us

$$\langle\overline{\cos^2\theta_D}\rangle = \frac{1}{2}\,\overline{\sin^2\theta_D'}\,\langle\sin^2\theta_D''\rangle + \overline{\cos^2\theta_D'}\,\langle\cos^2\theta_D''\rangle \tag{22}$$

An equivalent expression holds for $\langle\overline{\cos^2\theta_A}\rangle$.

Note that in this formulation it has not proven necessary to assume specific forms for the complete distributions of θ_D', θ_D'', θ_A', or θ_A''. The orientation factor is completely defined (as far as these angles are concerned) with the specification of only $\overline{\cos^2\theta_D'}$, $\langle\cos^2\theta_D''\rangle$, $\overline{\cos^2\theta_A'}$, and $\langle\cos^2\theta_A''\rangle$ and, hence, $\langle\overline{\cos^2\theta_D}\rangle$ and $\langle\overline{\cos^2\theta_A}\rangle$.

Figure 2 presents values of a_{VV}, a_{VH}, a_{HV}, and a_{HH} calculated as functions of θ_j for R = 125 Å with h ranging from 0 to 25 Å. For all $h \neq 0$, a_{VV} approaches 4.0 as θ_j approaches zero, as one would expect for two collinear dipoles. All other limits are similarly as one would predict from simple geometrical analysis (Eisinger & Dale, 1974). Figure 3a reproduces curves for a_{VV}, a_{VH}, a_{HV}, and a_{HH} for the single value of h = 20 Å, demonstrating the wide range of values that the orientation factor can assume in a specific case in the absence of dynamic averaging.

Figure 3b,c presents the corresponding curves (a_{VV}', a_{VH}', a_{HV}', and a_{HH}') calculated in the presence of dynamic averaging. The primed factors are averages of a_{VV}, a_{VH}, a_{HV}, and a_{HH}, weighted by functions of $\overline{\cos^2\theta_D'}$ and $\overline{\cos^2\theta_A'}$. They are defined such that $\langle\overline{\kappa_j^2}\rangle_{A_j}$ (combining eq 19 and 22) is expressed as an average of a_{VV}', a_{VH}', a_{HV}', and a_{HH}', weighted by functions of $\langle\cos^2\theta_D''\rangle$ and $\langle\cos^2\theta_A''\rangle$ (analogous to eq 19). Subscripts V and H, in this case, indicate vertical ($\langle\cos^2\theta''\rangle = 1$) and horizontal ($\langle\cos^2\theta''\rangle = 0$) *distributions* of transition dipoles. Dynamic averaging dramatically reduces the possible values to a limited range about 2/3, the value predicted for the limit of totally random orientations.[3] For random distributions of the acceptor (i.e., $\overline{\cos^2\theta_A'}$ and/or $\langle\cos^2\theta_A''\rangle$ and,

[3] As far as energy transfer is concerned, "random" orientation is synonymous to $\langle\overline{\cos^2\theta}\rangle = 1/3$. This can correspond to a distribution uniform on the surface of the unit sphere (i.e., $P(\theta)d\theta = 1/2 \sin\theta\, d\theta$) but is also consistent with a variety of anisotropic distributions [e.g., $P(\theta)d\theta = \delta[\theta - \cos^{-1}(1/3)^{1/2}]d\theta$].

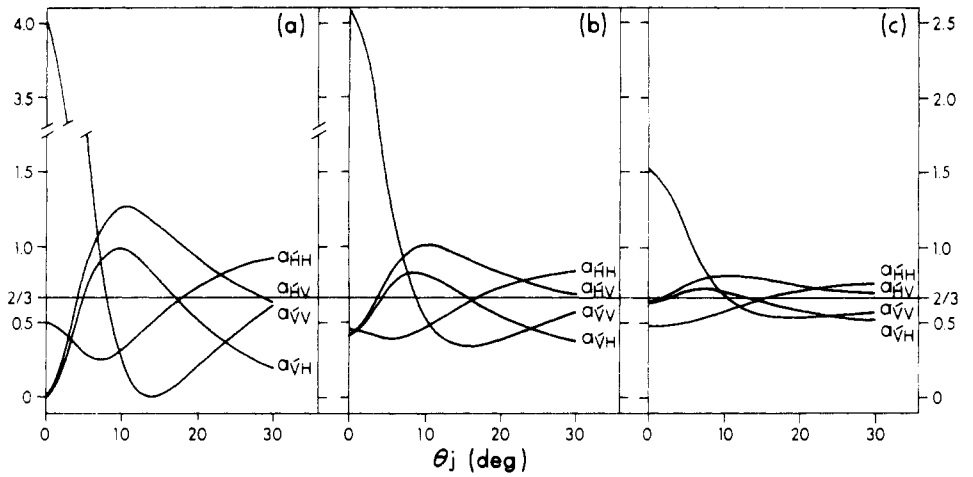

FIGURE 3: Theoretical curves of a_{VV}', a_{VH}', a_{HV}', and a_{HH}' presented for $h = 20$ Å, $R = 125$ Å, with $\overline{\cos^2 \theta_D'} = \overline{\cos^2 \theta_A'}$ = (a) 1.00; (b) 0.80; (c) 0.60. Case c represents an extent of dynamic averaging comparable to that observed by Fleming et al. (1979).

hence, $\langle \overline{\cos^2 \theta_A} \rangle = 1/3$) and the donor (i.e., $\overline{\cos^2 \theta_D'}$ and/or $\langle \cos^2 \theta_D'' \rangle$ and, hence, $\langle \overline{\cos^2 \theta_D} \rangle = 1/3$)

$$\langle \kappa_j^2 \rangle_{A_j} = \frac{1}{9}a_{VV} + \frac{2}{9}a_{VH} + \frac{2}{9}a_{HV} + \frac{4}{9}a_{HH} = \frac{2}{3}$$

exactly, for each and every value of R, h, and θ_j.

Finally, in the limit of a planar membrane ($R \gg h$), eq 20a–d reduce to

$$a_{VV} = (1 - 3z_j^2/r_j^2)^2 \tag{23a}$$

$$a_{VH} = a_{HV} = (9/2)z_j^2 y_j^2/r_j^4 \tag{23b}$$

$$a_{HH} = (1/4)[1 + (1 - 3y_j^2/r_j^2)^2] \tag{23c}$$

where now

$$y_j = (A_j/\pi)^{1/2}$$

$$z_j = h$$

A Useful Limiting Case. Expressions derived above simplify considerably if all donor–acceptor pairs are assumed to have the same orientation factor. In this case, we can define a single characteristic distance of transfer, R_0, such that

$$\langle \tilde{\gamma}_j \rangle_{A_j} = R_0^6/r_j^6 \tag{24}$$

In the limit expressed by eq 24, eq 9 is exactly equivalent to eq 25A to 26A of Shaklai et al. (1977) and eq 3 to 4 of Fung & Stryer (1978). In our notation, $\langle E \rangle$ is now a function of five parameters: h, A_{ex}, R, R_0, and σ. We can go further, however, and demonstrate that these five parameters appear in combinations that can be fully characterized with the specification of only two dimensionless parameters.

Evaluations of $\langle \rho(t) \rangle$ via eq 9 and 10 and $\langle E \rangle$ via eq 14 and 15 proceed with changes to the dimensionless integration variable $x_j \equiv \sigma(A_j - A_{ex})$. Thus, we have

$$\langle \rho(t) \rangle = \exp\left\{-t/\tau_0 - \int_0^\infty [1 - \exp(-\langle \tilde{\gamma}_j \rangle_{A_j} t/\tau_0)]\, dx_j\right\} \tag{25}$$

and

$$\langle E \rangle = \int_0^\infty \frac{\langle \Gamma \rangle_{A_1}}{1 + \langle \Gamma \rangle_{A_1}} e^{-x_1}\, dx_1 \tag{26}$$

with

$$\langle \Gamma \rangle_{A_1} = \langle \tilde{\gamma}_1 \rangle_{A_1} + \int_{x_1}^\infty \langle \tilde{\gamma}_j \rangle_{A_j}\, dx_j \tag{27}$$

It remains simply to evaluate $\langle \tilde{\gamma}_j \rangle_{A_j}$ as a function of x_j. Combining eq 3 and 24

$$\langle \tilde{\gamma}_j \rangle_{A_j} = \left(\frac{h^2}{R_0^2} + \frac{R-h}{R}\frac{A_{ex}}{\pi R_0^2} + \frac{R-h}{R}\frac{x_j}{\pi R_0^2 \sigma} \right)^{-3} = \left(r_0^2 + \frac{x_j}{n_0} \right)^{-3} \tag{28}$$

Examination of eq 25–28 reveals that, in either formulation, the net result of energy transfer is indeed a function of two dimensionless parameters:

$$r_0^2 = (r_{min}/R_0)^2 \tag{29}$$

where r_{min} is the distance of closest approach

$$r_{min} = \left(h^2 + \frac{R-h}{R}\frac{A_{ex}}{\pi} \right)^{1/2} \tag{30}$$

and n_0 is an effective number of acceptors

$$n_0 = \frac{R}{R-h}\pi R_0^2 \sigma \tag{31}$$

Physically, n_0 is the number of acceptors located, on average, at distances between r_j and $(r_j^2 + R_0^2)^{1/2}$ for all possible values of r_j. The effect of vesicle curvature is contained in the factor $R/(R-h)$ in n_0 and r_0^2. If $h > 0$, vesicle curvature acts to increase the transfer efficiency by bringing acceptors closer to the donor. If $h = 0$, $\langle E \rangle$ is independent of curvature.

Equation 25 can be evaluated further. Changing variables to $\xi \equiv \langle \tilde{\gamma}_j \rangle_{A_j} t/\tau_0$ and integrating by parts, we have

$$\langle \rho(t) \rangle = \exp\left\{ -\frac{t}{\tau_0} - n_0 \left[\tilde{\gamma}\left(\frac{2}{3}, \xi_0\right) - \xi_0^{-1/3}(1 - e^{-\xi_0}) \right] \left(\frac{t}{\tau^0}\right)^{1/3} \right\} \tag{32}$$

where

$$\xi_0 = r_0^{-6} t/\tau_0 \tag{33}$$

and

$$\tilde{\gamma}(\mu, \nu) = \int_0^\nu e^{-t} t^{\mu-1}\, dt \tag{34}$$

is the incomplete γ function [see, for example, Davis (1965)].

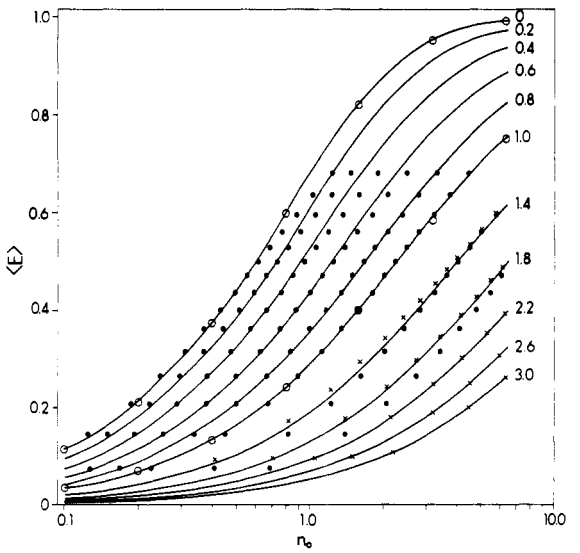

FIGURE 4: $\langle E \rangle$ as functions of n_0 for several discrete values of r_0^2 (as indicated next to each curve). Continuous curves were calculated directly via eq 26–28. (○) $\langle E \rangle$ calculated from $\langle \rho(t) \rangle$ via eq 6 and 32–34; (×) $\langle E \rangle$ in limit of $r_0^6 \gg 1$ according to eq 38; (●) empirical fit to theory (eq 39 to 40).

Equation 32 reduces to simple analytical forms in two important limits. When r_{min}^6 is much less than R_0^6

$$\lim_{r_0^6 \to 0} \langle \rho(t) \rangle = \exp\left[-\frac{t}{\tau_0} - n_0 \Gamma\left(\frac{2}{3}\right)\left(\frac{t}{\tau_0}\right)^{1/3} \right] \quad (35)$$

where

$$\Gamma\left(\frac{2}{3}\right) = \int_0^\infty e^{-t} t^{-1/3}\, dt = 1.354... \quad (36)$$

Transfer introduces a new term proportional to $(t/\tau_0)^{1/3}$. An equivalent expression has been derived by Tweet et al. (1964) for a planar array. The analogous expression for donors and acceptors in three-dimensional solution contains a term proportional to $(t/\tau_0)^{1/2}$ (Förster, 1949).

When r_{min}^6 is much greater than R_0^6

$$\lim_{r_0^6 \to \infty} \langle \rho(t) \rangle = \exp\left[-\left(1 + \frac{n_0}{2r_0^4} \right)\frac{t}{\tau_0} \right] \quad (37)$$

$\langle \rho(t) \rangle$ remains a single exponential. This is the limit considered by Shaklai et al. (1977) for a planar geometry. By eq 6, one then has the simple form for ⟨E⟩ of

$$\langle E \rangle = \frac{n_0/2r_0^4}{1 + n_0/2r_0^4} \quad (38)$$

Equation 38 can also be derived directly from eq 7, assuming a homogeneous continuum of acceptors.

Figure 4 presents $\langle E \rangle$ as a function of n_0 for several discrete values of r_0^2. The continuous curves were calculated directly from eq 26–28. The large open circles were calculated via eq 6 by using the functional forms of eq 32–34. The x's are values of $\langle E \rangle$ according to eq 38. These results confirm the equivalence of the two approaches to the problem presented here, demonstrating that, to a high degree of accuracy, the array of acceptors can be represented as consisting of a single nearest acceptor plus a continuum of secondary acceptors.

Data Analysis

In general, $\langle E \rangle$, as formulated above, is a function of h, A_{ex}, R, σ, β, $\overline{\cos^2 \theta_D'}$, $\overline{\cos^2 \theta_A'}$, $\langle \cos^2 \theta_D'' \rangle$, and $\langle \cos^2 \theta_A'' \rangle$. In most cases, R, β, $\overline{\cos^2 \theta_D'}$, and $\overline{\cos^2 \theta_A'}$ will be known. $\langle E \rangle$ is relatively insensitive to R, so that there is usually little difficulty in estimating R with sufficient accuracy. β can be accurately computed from known spectroscopic properties of the fluorescent probes. $\overline{\cos^2 \theta_D'}$ and $\overline{\cos^2 \theta_A'}$ can be estimated from fluorescence polarization data by using the relationship of eq 49 (Dale et al., 1979). Generally, one will want to determine σ for a given h and A_{ex} or, conversely, determine h and A_{ex} for a given σ. This latter strategy is emphasized here and in the following paper (Fleming et al., 1979). $\langle \cos^2 \theta_D'' \rangle$ and $\langle \cos^2 \theta_A'' \rangle$, most likely will not be known or determined. In the final analysis, they can be varied over the range of possible values as a means of assessing the uncertainty of other parameters.

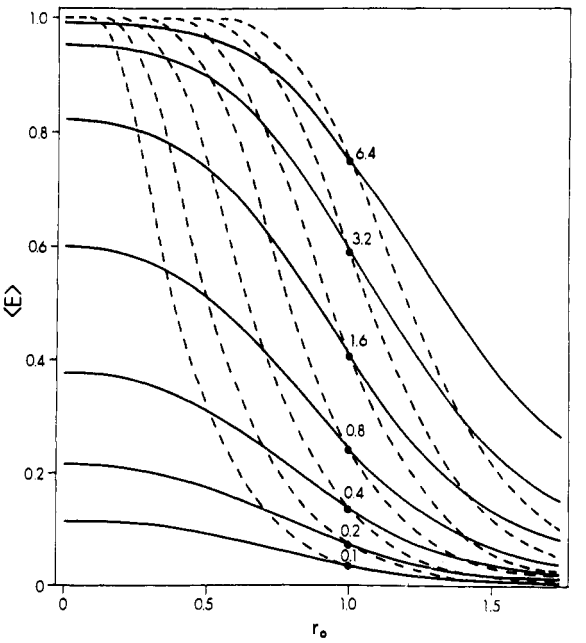

FIGURE 5: $\langle E \rangle$ as functions of r_0 for several discrete values of n_0 (solid lines) and $n_0 r_0^2$ (dashed lines). Numbers at crossover points at $r_0 = 1$ indicate specific values of n_0 and $n_0 r_0^2$.

Before we consider specific procedures of data analysis, it would be advantageous to discuss the conditions needed to maximize the sensitivity of the measurement of the parameter in question. The determination of σ is relatively straightforward. Maximal sensitivity, i.e., maximal values of $d\langle E \rangle/d\sigma$, will be achieved if R_0 and/or r_{min} are such that $\langle E \rangle$ spans 0.5 for the range of σ being considered. For very low surface densities one should thus seek to maximize R_0 and minimize r_{min}. R_0 and r_{min} can be adjusted in principle with artful selections of the donor and acceptor chromophores. In any event, examination of Figure 4 reveals that for a wide range of $\langle E \rangle$ ($0.2 \lesssim \langle E \rangle \lesssim 0.8$), $\langle E \rangle$ is a sensitive function of σ for all combinations of r_0 and n_0.

The conditions needed for accurate determinations of r_{min} are more complex. The solid lines in Figure 5 are graphs of $\langle E \rangle$ as functions of r_0 for several discrete values of n_0. It can be seen that for all values of n_0, and, hence, all values of ⟨E⟩, $\langle E \rangle$ is insensitive to r_0 for all $r_0 < 0.5$. Faced with this situation, one should seek to decrease R_0 and thus achieve a higher value of r_0 for the value of r_{min} in question. Near optimal sensitivity, i.e., maximal values of $d\langle E \rangle/dr_0$, will be achieved when $r_0 \simeq 1$, for $1 \lesssim n_0 \lesssim 5$. For a given accessible range of σ, however, decreasing R_0 will decrease the accessible range of n_0. Thus, the lower limit of r_{min} that can be determined with precision is fundamentally limited by σ_{max}, the maximum value of σ. This relationship can be put on a firm basis with consideration of the parameter $n_0 r_0 \simeq \pi r_{min}^2 \sigma$. This parameter,

evaluated at σ_{max}, defines the accessible ranges of r_0 and n_0. The dashed lines in Figure 5 are contours of constant values of $n_0 r_0^2$. These contours map out the values that $\langle E \rangle$ assumes as R_0 is varied for constant values of r_{min} and σ. At each value of r_0, one has access to all values of n_0 lying beneath the contour corresponding to $\pi r_{min}^2 \sigma_{max}$. It can thus be estimated that one can make reasonably accurate determinations of r_{min} whenever $\pi r_{min}^2 \sigma_{max} \gtrsim 0.5$. For smaller values of r_{min}, one may have to be content with calculations of estimated upper limits.

We have found a two-stage plan of data analysis to be advantageous. In the first stage, the data are fit to the simplified theory in which it is assumed that $\langle \overline{\kappa_j^2} \rangle_{A_j} = 2/3$. As Figure 3 demonstrates, this is likely to be a reasonably good approximation. To facilitate the first stage of analysis, we have derived an empirical fit to $\langle E \rangle$ as a function of r_0 and n_0. We have found that the form

$$\langle E \rangle = \frac{(n_0/n_0^{50\%})^{1.10}}{1 + (n_0/n_0^{50\%})^{1.10}} \tag{39}$$

with

$$n_0^{50\%} = 0.62 \exp(-0.34 r_0 + 1.63 r_0^2) \tag{40}$$

gives a good representation for useful ranges of r_0 and n_0. The series of small solid circles on Figure 4 are values of $\langle E \rangle$ calculated with eq 39 and 40. Undoubtedly, a functional form could be found which would give a still better fit over a wider range. The advantage here is that of analytical simplicity. Combined with eq 31, one can solve directly for r_0 as a function of R_0, σ, $\langle E \rangle$, h, and R:

$$r_0 = 0.10 + \left\{0.011 + 0.61 \ln\left[1.61 \frac{R}{R-h} \pi R_0^2 \sigma \left(\frac{1-\langle E \rangle}{\langle E \rangle}\right)^{0.91}\right]\right\}^{1/2} \tag{41}$$

Thus, if R_0, σ, $\langle E \rangle$, and R are known, one can calculate r_{min} and A_{ex} for assumed values of h. Since, in general, R will be much greater than h, r_{min} calculated via eq 41 will be practically independent of the assumed value of h. Thus, without additional information, one will have an unambiguous estimate of r_{min}. If one can by other considerations put limits on the possible range of A_{ex}, then correspondingly one will put limits on the possible value of h. An example of such a procedure is presented in the following paper (Fleming et al., 1979).

Similarly, one can solve for σ as a function of r_0, R_0, $\langle E \rangle$, h, and R:

$$\sigma = \frac{0.62}{\pi R_0^2} \frac{R-h}{R} \left(\frac{\langle E \rangle}{1-\langle E \rangle}\right)^{0.91} \exp(-0.34 r_0 + 1.63 r_0^2) \tag{42}$$

Note that, for relatively small values of r_{min} or large values of R_0 ($R_0 > 3r_{min}$), the value of σ calculated via eq 42 is virtually independent of r_0, as would be expected.

Results derived via eq 41 or 42 can be checked with calculations of $\langle E \rangle$ based on the general formulation, incorporating the effects of uncertainties in the value of the orientation factor. $\langle E \rangle$ is calculated via eq 6, 9, and 10, or 14 and 15, by using the general expression for $\langle \overline{\kappa_j^2} \rangle_{A_j}$ (eq 19, 20, and 22). The extent of dynamic averaging, contained in the factors $\overline{\cos^2 \theta_D'}$ and $\overline{\cos^2 \theta_A'}$, is estimated from polarization data [see Fleming et al. (1979)]. The possible range of $\langle \overline{\kappa_j^2} \rangle_{A_j}$, and, hence, the possible range of $\langle E \rangle$, is covered by systematically varying the ensemble averaging parameters, $\langle \cos^2 \theta_D'' \rangle$ and $\langle \cos^2 \theta_A'' \rangle$, between 0 and 1 (see eq 22). The values of $\langle E \rangle$ thus obtained will center about those corresponding to a uniform $\langle \overline{\kappa_j^2} \rangle_{A_j} = 2/3$. The complete formulation will help place reasonable uncertainties on these results.

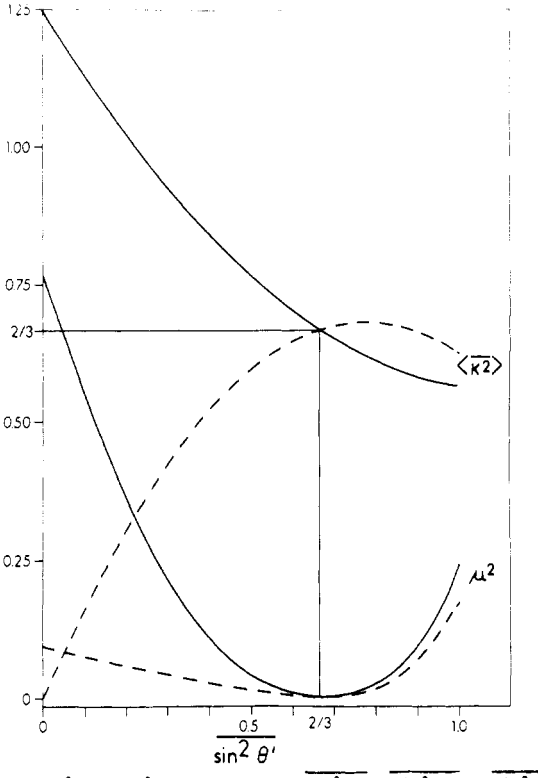

FIGURE 6: $\langle \kappa^2 \rangle$ and μ^2 as functions of $\overline{\sin^2 \theta'} = \overline{\sin^2 \theta_D'} = \overline{\sin^2 \theta_A'}$. Solid curves correspond to case I (eq 3A and 4A). Dashed curves correspond to case II (eq 5A and 6A).

Appendix

Evaluation of Correction Terms. In the derivations of the basic eq 9, 10, and 14, second-order and higher order terms in Taylor expansion were discarded. Physically, this was equivalent to assuming that all averaging over the orientations of the donor and acceptor transition dipoles occurs as dynamic averaging. When orientations are dynamically averaged, dipoles initially in an orientation unfavorable for transfer have time to assume a more favorable orientation during the donor excited-state lifetime. The net result is an increased efficiency of transfer. Thus, in general, eq 9 (substituting the first term from eq 10) and 14 will overestimate $\langle E \rangle$. It is important at this time to estimate the magnitude of this effect.

The first nonzero correction terms from the Taylor expansions are proportional to μ_j^2, the normalized ensemble averaged second moment of $\overline{\kappa_j^2}$ about the ensemble average. Since it is not practical to derive a general expression for μ_j^2 as was done for $\langle \overline{\kappa_j^2} \rangle_{A_j}$, we turn instead to simple, specific, but representative cases. Consider an array of donors and acceptors at the same level (i.e., $h = 0$) in a planar membrane. For this geometry, it is rigorously true that $\langle \overline{\kappa_j^2} \rangle_{A_j}$ is identical for each donor–acceptor pair, independent of A_j, as was assumed in a previous section. Including the first correction term, we now have, in the notation of eq 32

$$\langle \rho(t) \rangle = \exp\left\{-\frac{t}{\tau_0} - n_0\left[\bar{\gamma}\left(\frac{2}{3}, \xi_0\right)(1 - \mu^2/9) + \xi_0^{-1/3}(1 - e^{-\xi_0}) - \frac{\mu^2}{6}\xi_0^{2/3} e^{-\xi_0}\right]\left(\frac{t}{\tau_0}\right)^{1/3}\right\} \tag{1A}$$

In the limit of $r_{min}^6 \ll R_0^6$, which will surely be true with $h = 0$

$$\lim_{r_0^6 \to 0} \langle \rho(t) \rangle = \exp\left[-\frac{t}{\tau_0} - n_0 \Gamma\left(\frac{2}{3}\right)(1 - \mu^2/9)\left(\frac{t}{\tau_0}\right)^{1/3} \right] \tag{2A}$$

Thus, in this case, the correction term has an effect equivalent to that of reducing the value of n_0 by a factor of $(1 - \mu^2/9)$. It only remains now to compute explicit numerical values for μ^2.

Calculation of μ^2 procedes analogously to that presented above for $\langle \overline{\kappa_j^2} \rangle_{A_i}$. We present the results for two specific cases. (I) $\hat{z}_D'$ and $\hat{z}_A'$ in the plane of the membrane; i.e., $\cos \theta_D'' = \cos \theta_A'' = 0$. In this case

$$\langle \overline{\kappa^2} \rangle = \frac{5}{4} - \frac{5}{8}(\overline{\sin^2 \theta_D'} + \overline{\sin^2 \theta_A'}) + \frac{9}{16} \overline{\sin^2 \theta_D'}\ \overline{\sin^2 \theta_A'} \tag{3A}$$

and

$$\langle (\delta\overline{\kappa^2})^2 \rangle = \frac{77}{64} - \frac{195}{64}(\overline{\sin^2 \theta_D'} + \overline{\sin^2 \theta_A'}) + \frac{477}{64} \overline{\sin^2 \theta_D'}\ \overline{\sin^2 \theta_A'} + \frac{549}{256}[(\overline{\sin^2 \theta_D'})^2 + (\overline{\sin^2 \theta_A'})^2] - \frac{1323}{256}[\overline{\sin^2 \theta_D'}\ (\overline{\sin^2 \theta_A'})^2 + (\overline{\sin^2 \theta_D'})^2\ \overline{\sin^2 \theta_A'}] + \frac{3645}{1024}(\overline{\sin^2 \theta_D'})^2\ (\overline{\sin^2 \theta_A'})^2 \tag{4A}$$

(II) $\hat{z}_D'$ perpendicular to the plane of the membrane, $\hat{z}_A'$ in the plane of the membrane; i.e., $\cos \theta_D'' = 1$ and $\cos \theta_A'' = 0$. In this case

$$\langle \overline{\kappa^2} \rangle = \frac{1}{2} \overline{\sin^2 \theta_A'} + \frac{5}{4} \overline{\sin^2 \theta_D'} - \frac{9}{8} \overline{\sin^2 \theta_D'}\ \overline{\sin^2 \theta_A'} \tag{5A}$$

and

$$\langle (\delta\overline{\kappa^2}) \rangle = \frac{9}{32} (\overline{\sin^2 \theta_D'})^2 - \frac{27}{32} (\overline{\sin^2 \theta_D'})^2\ \overline{\sin^2 \theta_A'} + \frac{81}{128} (\overline{\sin^2 \theta_D'})^2\ (\overline{\sin^2 \theta_A'})^2 \tag{6A}$$

The case of $\cos \theta_D'' = 0$ and $\cos \theta_A'' = 1$, obviously, is equivalent to II. One need only interchange θ_D' and θ_A'. If $\cos \theta_D'' = \cos \theta_A'' = 1$, on the other hand, there is no static averaging at all and $\mu^2 = 0$.

Figure 6 presents calculated values of $\langle \overline{\kappa^2} \rangle$ and μ^2 as functions of $\overline{\sin^2 \theta_D'} = \overline{\sin^2 \theta_A'}$, i.e., as functions of the extent of dynamic averaging. Note that, with dynamic averaging over uniform distributions of θ_D' and θ_A', a situation corresponding to $\overline{\sin^2 \theta_D'} = \overline{\sin^2 \theta_A'} = 2/3$, one has $\langle \overline{\kappa^2} \rangle = 2/3$ and $\mu^2 = 0$, as expected. For the amount of dynamic averaging considered in the following paper (Fleming et al., 1979), $\mu^2/9$ is limited to no more than a few percent, in either case, and can safely be neglected.

References

Dale, R. E., & Eisinger, J. (1974) Biopolymers *13*, 1573–1605.

Dale, R. E., Eisinger, J., & Blumberg, W. E. (1979) *Biophys. J. 26*, 161–194.

Davis, P. J. (1965) in *Handbook of Mathematical Functions* (Abramowitz, M., & Stegun, I. A., Eds.) pp 255–293, Dover Publications, New York.

Eisinger, J., & Dale, R. E. (1974) *J. Mol. Biol. 84*, 643–647.

Fleming, P. J., Koppel, D. E., Lau, A. L. Y., & Strittmatter, P. (1979) *Biochemistry* (following paper in the issue).

Förster, T. (1948) *Ann. Phys. (Leipzig) 2*, 55–75.

Förster, T. (1949) *Z. Naturforsch. 4A*, 321–327.

Fung, B. K.-K., & Stryer, L. (1978) *Biochemistry 17*, 5241–5248.

Haas, E., Katchalski-Katzir, E., & Steinberg, I. Z. (1978) *Biochemistry 17*, 5064–5070.

Shaklai, N., Yguerabide, J., & Ranney, H. M. (1977) *Biochemistry 16*, 5585–5592.

Stryer, L. (1978) *Annu. Rev. Biochem. 47*, 819–846.

Tweet, A. G., Bellamy, W. D., & Gaines, G. L., Jr. (1964) *J. Chem. Phys. 41*, 2068–2077.